Article:
Parlett, CMA, Durndell, LJ, Wilson, K et al. (3 more authors) (2014) Selective oxidation of allylic alcohols over highly ordered Pd/meso-Al2O3 catalysts. Catalysis Communications, 44. 40 - 45. ISSN 1566-7367

https://doi.org/10.1016/j.catcom.2013.07.005

Selective oxidation of allylic alcohols over highly ordered Pd/meso-Al_2O_3 catalysts

Christopher M.A. Parlett,[1] Lee J. Durndell,[1] Karen Wilson,[1] Duncan W. Bruce,[2] Nicole S. Hondow,[3] Adam F. Lee.[1]

1. Cardiff Catalysis Institute, School of Chemistry, Cardiff University, Cardiff CF10 3AT, UK

2. Department of Chemistry, University of York, Heslington, York YO10 5DD, UK

3. Institute for Materials Research, School of Process, Environmental and Materials Engineering, University of Leeds, Leeds, LS2 9JT, UK

Abstract

Highly ordered mesoporous alumina was prepared via evaporation induced self-assembly and was impregnated to afford a family of Pd/meso-Al_2O_3 catalysts for the aerobic selective oxidation (selox) of allylic alcohols under mild reaction conditions. CO chemisorption and XPS identify the presence of highly dispersed (0.9–2 nm) nanoparticles comprising heavily oxidised PdO surfaces, evidencing a strong palladium-alumina interaction. Surface PdO is confirmed as the catalytically active phase responsible for allylic alcohol selox, with initial rates for Pd/meso-Al_2O_3 far exceeding those achievable for palladium over either amorphous alumina or mesoporous silica supports. Pd/meso-Al_2O_3 is exceptionally active for the atom efficient selox of diverse allylic alcohols, with activity inversely proportional to alcohol mass.

1. Introduction

The drive towards greener and more sustainable chemicals manufacture requires the development of new synthetic protocols and processes, offering enhanced atom-economy and energy efficiency [1]. In this respect, the green synthesis of allylic aldehydes, an important class of polyfunctional chemical intermediates that find widespread application in the agrochemical, fragrance/flavourings and pharmaceutical sectors, has been the focus of intense academic and commercial research, with the direct, aerobic selective oxidation (selox) of the corresponding alcohol derivatives offering a low temperature, low cost and clean approach [2]. By this means, cinnamaldehyde, an insecticide [3] and common food/perfume additive can be obtained via cinnamyl alcohol from the leaves of Cinnamomum verum. Other naturally occurring allylic alcohols, whose aldehyde derivatives are valuable chemical intermediates, include prenol (genus citrus) and geraniol (genus Rosa and Cymbopogon): citral, a product of geraniol selox, shows appreciable antimicrobial activity against diverse micro-organisms [3] and is a precursor in the commercial synthesis of vitamin A [4] and [5], while crotonaldehyde is a precursor to the food preservative sorbic acid [5].

Heterogeneous, late transition metal catalysts, notably gold and palladium, are particularly active for the liquid and vapour phase aerobic selox of allylic alcohols [2], with catalyst performance a strong function of the metal electronic structure and support textural properties. We have extensively investigated the behaviour of Pd nanoparticles on mesoporous silica supports, wherein high activities for crotyl and cinnamyl alcohol selox towards crotonaldehyde and cinnamaldehyde respectively are possible through tuning the mesopore architecture [6] and [7]. Detailed kinetic investigations, alongside in situ [8], [9] and [10] and operando studies [11], [12], [13] and [14] have provided conclusive evidence that allylic alcohol oxidation occurs via a redox mechanism, catalysed by electron deficient, surface Pd(II) species present as PdO. Kumar et al. [15], Scott et al. [16] and Hara et al. [17] have likewise reported a heterogeneous Pd(II) active species

responsible for aerobic alcohol selox, while homogeneous Pd(II) complexes are well known to catalyse such alcohol oxidations [18], [19] and [20]. Interestingly, surface PtO2 has also been recently reported as the active phase in the analogous Pt catalysed aerobic selox of allylic alcohols [21].

Surface oxidation of palladium nanoparticles is a strong (inverse) function of their attendant particle size, hence low Pd loadings favour highly dispersed and heavily oxidised palladium. However, a key barrier to the commercialisation of Pd selox catalysts is their on-stream deactivation via in situ reduction to metallic palladium, even under atmospheric pressures of oxygen or air. In part, this reflects the weak interaction of palladium with (non-reducible) silica supports largely employed to date, necessitating recourse to high surface area forms of silica with complex, interconnecting architectures [6] and [7]. Amino-functionalised silica supports offer one route to help stabilise highly dispersed Pd nanoparticles [22], [23] and [24], but require additional preparative steps, generating associated waste, and narrow the pore dimensions hindering intra-pore mass transport. An alternative approach to stabilising highly dispersed palladium is to select a support material with a greater affinity for the element, such as alumina [25] or silica-alumina [26], wherein Al-rich supports favour sub-2 nm (or even atomically-dispersed) palladium.

In contrast to silicas and carbons, the synthesis of high surface area mesostructured aluminas is relatively undeveloped, with early surfactant-templating approaches employing carboxylic acids achieving high surface areas (760 m^2g^{-1}), but small (2 nm diameter) randomly ordered mesopores [27]. Large mesopore (10 nm diameter) γ-alumina has been fabricated through the use of room temperature ionic liquids as a co-solvent and template; however this material comprises randomly debundled nanofibres embedded in a wormlike porous network, and hence presents a disordered environment for the preparation of uniformly dispersed catalytic centres and reactant/product diffusion. Evaporation-induced self-assembly (EISA) utilising poly(alkylene oxide) block copolymers affords a simple route to highly ordered 2D hexagonal (p6mm) mesoporous materials [28], and has been successfully applied to synthesise ordered mesoporous aluminas with high thermal stability [29] and [30], large pores up to 7.5 nm [31], diverse transition metal dopants [32] and [33], or hierarchical architectures containing complementary macropores via colloidal crystal co-templating with polystyrene microspheres [34].

Here we exploit the EISA route to produce a high surface area, highly ordered mesoporous alumina in order to stabilise dispersed palladium nanoparticles in an oxidised form, with the goal of enhancing the selective oxidation of allylic alcohols. The resulting Pd/meso-Al_2O_3 catalysts are active towards diverse allylic alcohols, and exhibit significantly higher turnover frequencies (TOFs) than their silica counterparts, with initial rates inversely proportional to palladium loading, reflecting a higher density of surface PdO active species and stronger Pd-alumina interaction.

2. Experimental

2.1. Mesoporous alumina synthesis

Highly ordered mesoporous alumina (meso-Al_2O_3) was prepared adopting the procedure of Yuan and co-workers [29]. Pluronic P123 surfactant (3 g, Sigma-Aldrich) was dissolved in anhydrous ethanol (60 cm^3, Sigma-Aldrich > 99.5%) under agitation, and nitric acid (4.5 cm^3, Fisher Scientific 65 wt%) and aluminium isopropoxide (6.2 g, Sigma-Aldrich 98%) subsequently added under stirring until dissolved and the mixture aged for 5 h. EISA was initiated by slow ethanol removal upon heating at 60 °C under static conditions. After

96 h, the resulting yellow solid was ground to a fine powder, and then heated at 0.4 °C min^{-1} under flowing O_2 (50 cm^3min^{-1}) to 600 °C for 3 h.

2.2. Pd impregnation

Palladium incorporation was achieved via incipient-wetness impregnation. Mesoporous alumina (1.5 g) was saturated with aqueous tetraammine palladium(II) nitrate solution (1.5 cm^3, with Pd concentrations adjusted to achieve nominal loadings spanning 0.05–5 wt% Sigma-Aldrich 10 wt%) at room temperature. The resulting slurries were stirred for 18 h before heating to 50 °C. Agitation was stopped after approximately 5 h, and the residual solids left to dry for 24 h at 50 °C. The dry powders were subsequently heated in static air at 1 °C min− 1 to 500 °C for 2 h, prior to heating at 10 °C min− 1 to 400 °C for 2 h under flowing H_2 (10 cm^3min^{-1}). Samples were then cooled to room temperature and stored in air. A nominal 1 wt% Pd on commercial Degussa C γ-alumina (surface area 180 m^2g^{-1}) was also prepared following the same protocol.

2.3. Materials characterisation

Nitrogen porosimetry was performed on a Quantachrome Nova 1200 porosimeter using NovaWin 2 v2.2 analysis software. Samples were degassed at 120 °C for 2 h prior to N_2 physisorption. Powder X-ray diffraction (XRD) patterns were recorded on a PANalytical X'Pert PRO diffractometer fitted with an X'Celerator detector, using a Cu Kα (1.54 Å) excitation source, with patterns calibrated against a Si standard. Transmission electron microscopy (TEM) and high angle annular dark field scanning transmission electron microscopy (HAADF STEM) images were recorded on a FEI Tecnai F20 FEG TEM operated at 200 kV and equipped with a Gatan Orius SC600A CCD camera. Samples were prepared by dispersion in methanol and drop-casting onto a copper grid coated with a holey carbon support film (Agar Scientific Ltd). Images were analysed using ImageJ 1.41 software. Actual Pd loadings were determined by MEDAC Analytical and Chemical Consultancy Service Ltd, with samples digested in HF prior to ICP analysis. X-ray photoelectron spectroscopy (XPS) was performed on a Kratos Axis HSi X-ray photoelectron spectrometer fitted with a charge neutralizer and magnetic focusing lens, using monochromated Al Kα radiation (1486.6 eV). Spectral fitting was performed with CasaXPS version 2.3.14. Binding energies were referenced to the adventitious C 1 s peak at 284.6 eV. Pd 3d XP spectra were fitted adopting a common asymmetric peak shape determined from that of a palladium oxide standard, and a spin-orbit doublet separation of 5.3 eV in agreement with literature values from the NIST surface database. Pd dispersion was measured via CO pulse chemisorption on a Quantachrome ChemBET 3000 system. Samples were outgassed at 150 °C under flowing He (20 cm^3min^{-1}) for 1 h, prior to reduction at 100 °C under flowing hydrogen (20 cm^3min^{-1}) for 1 h before analysis at room temperature.

2.4. Allylic alcohol selox

Catalyst screening was performed using a Radleys Starfish carousel batch reactor on a 10 cm^3 scale at 90 °C under a bubbled O_2 flow (3 cm^3min^{-1} at 1 bar). Catalyst (50 mg) was added to a reaction mixture of allylic alcohol (8.4 mmol, Sigma-Aldrich purity of all > 95%), mesitylene (0.1 cm^3, Sigma-Aldrich 99%) as an internal standard, and toluene (10 cm^3, Fisher Scientific 99.8%). Control reactions in the absence of any solid phase or presence of bare alumina supports, were conducted in parallel with tests on Pd/meso-Al_2O_3 and gave negligible conversion of any alcohols. Reactions were periodically sampled, with aliquot (0.25 cm^3) withdrawn, filtered, and diluted with toluene (1.75 cm^3, Fisher Scientific 99.8%) for triplicate analysed on a Varian 3900GC with CP-8400 autosampler (CP-Sil5 CB column, 15 m x 0.25 mm x 0.25 µm). Initial rates were calculated from the initial linear region of the alcohol conversion profiles (typically 0.3–1 h reaction), with

selectivity and overall mass balances calculated using calibrated response factors for reactants and products. Conversion and selectivity values are reported within ± 3 % error, with mass balances in all cases ≥ 95 % during the first hour and ≥ 90 % over 24 h. Catalyst recyclability was assessed by screening a spent quantity of catalysts from a scaled-up (by a factor of 2.5) to ensure significant catalyst recovery by hot filtration. Spent catalysts were stirred in 50 ml toluene at 90 °C for 10 min (three times) before drying at 120 °C for 2 h and subsequent catalytic testing under identical conditions to those stated above.

3. Results and discussion

3.1. Catalyst characterisation

The successful synthesis of alumina possessing a p6mm 2D hexagonally packed, cylindrical pore architecture (meso-Al_2O_3) with a high degree of mesopore ordering is evidenced in Fig. 1. Low-angle XRD confirmed a p6mm mesostructure, which was readily visualised by TEM (see also Fig. S1). Textural properties were in good agreement with the literature [29], with meso-Al_2O_3 exhibiting a mean pore diameter of 6.5 nm, a type IV nitrogen adsorption isotherm and type H1 hysteresis characteristic of independent, cylindrical mesopores, and surface area of 280 m^2g^{-1} (Table S1).

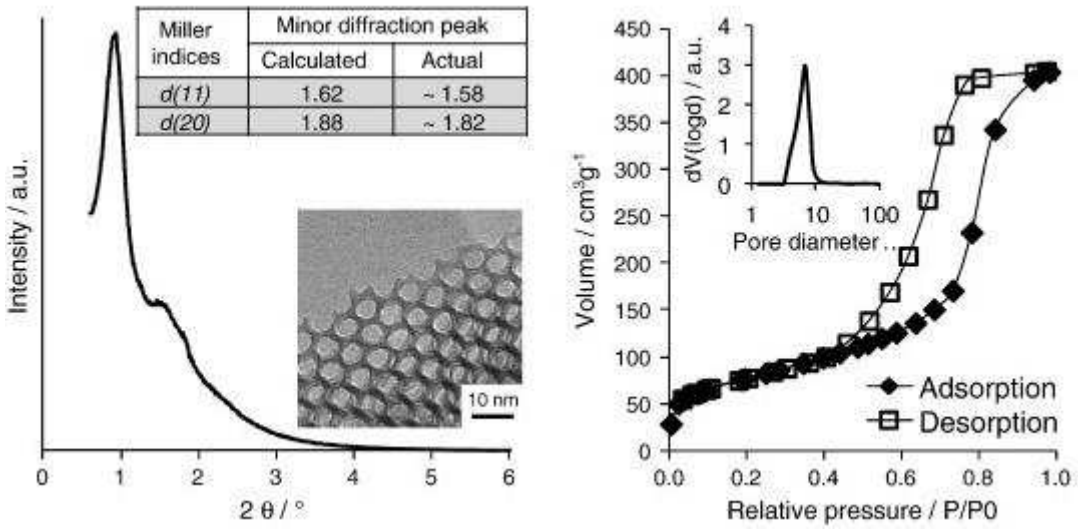

Fig. 1. (Left) Low-angle XRD pattern and TEM micrograph of parent meso-Al_2O_3; and (right) corresponding adsorption/desorption isotherms and inset BJH pore size distribution.

Subsequent palladium impregnation resulted in a family of Pd/meso-Al_2O_3 materials with bulk Pd loadings spanning 0.05–4.11 wt%. HAADF STEM images of the 0.74 wt% Pd/meso-Al_2O_3 sample in Fig. 2 show the presence of well-distributed Pd nanoparticles with a relatively narrow size distribution and mean diameter of 1.1 (± 0.5) nm.

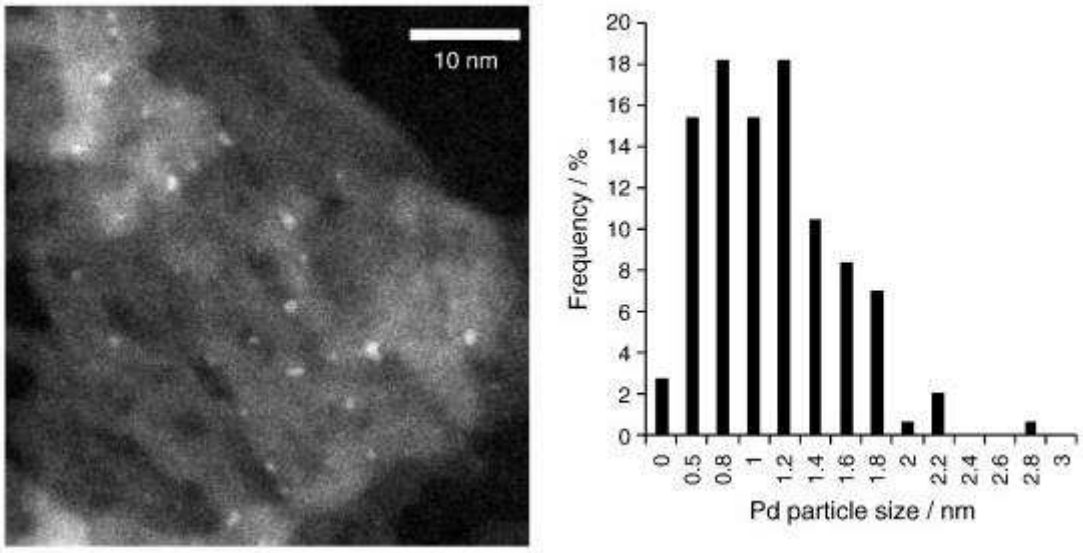

Fig. 2. (Left) HAADF-STEM micrograph of 0.74 wt% Pd/meso-Al_2O_3; and (right) corresponding Pd nanoparticle size distribution.

Palladium dispersions, and corresponding mean particle sizes, were estimated via CO chemisorption and are presented in Table 1: these respectively increase from 63 % to 93 % and decrease from 1.8 to 0.9 nm with falling palladium loading, consistent with the concomitant rise in palladium surface oxidation observed by XPS (Fig. S2) from 9 % PdO (4.11 wt% Pd/meso-Al_2O_3) to 50 % PdO (0.05 wt% Pd/meso-Al_2O_3). The degree of surface oxidation compares favourably with that attainable over mesoporous silicas, for which maxima of only 25 % and 34 % PdO were observed over higher area SBA-15 and KIT-6 supports respectively [6] and [7], indicating that alumina is indeed better able to stabilise palladium in a higher oxidation state than silica as hoped due to a stronger metal-support interaction [35].

Support	Pd loading[(a)] /wt%	Dispersion[(b)] /%	Ave. particle size[(b)] /nm	PdO content[(c)] /%
meso-Al_2O_3	4.11	63 (± 1)	1.8 (± 0.1)	8.7 (± 0.9)
meso-Al_2O_3	1.75	67 (± 1)	1.7 (± 0.1)	14.9 (± 1.5)
meso-Al_2O_3	0.74	74 (± 1)	1.5 (± 0.1)	21.9 (± 2.2)
meso-Al_2O_3	0.44	84 (± 1)	1.2 (± 0.1)	28.1 (± 2.8)
meso-Al_2O_3	0.07	88 (± 2)	0.1 (± 0.1)	44.4 (± 4.4)
meso-Al_2O_3	0.05	93 (± 5)	0.9 (± 0.1)	49.9 (± 5.0)
γ-Al_2O_3	0.79	68 (± 1)	1.7 (± 0.1)	14.4 (± 1.4)
SBA-15[(d)]	0.89	52 (± 1)	2.3 (± 0.1)	6.0 (± 0.6)
KIT-6[(d)]	0.78	71.5 (± 1)	1.6 (± 0.1)	11.3 (± 1.1)

Table 1. Comparative structural properties of Pd nanoparticles over alumina and silica supports. (a) ICP-OES, (b) CO chemisorption using average CO:Pd stoichiometry of 1:2, (c) % PdO from fitted Pd 3d XP spectra, (d) From Ref. [6] and [7].

3.2. Allylic alcohol selox

The performance of our highly ordered Pd/meso-Al_2O_3 family was first benchmarked against cinnamyl alcohol selox for comparison with our previously reported Pd/meso-silicas [6] and [7]. All Pd loadings exhibited excellent activity profiles (Fig. S3) under the mild reaction condition employed (90 °C and 1 bar O_2).

For palladium on silica supports, such as amorphous silica gel, SBA-15, SBA-16 or KIT-6, the initial rate of cinnamyl alcohol selox slows with increasing Pd loading due to a corresponding rapid decline in surface PdO concentration. Similar behaviour is seen for the present Pd/meso-Al_2O_3 catalysts (Fig. 3), however the initial rates are far superior to those obtained even over the most active silica counterpart published to date, with a maximum rate of 73,960 mmol gPd^{-1} h^{-1} for 0.05 wt% Pd-meso-Al_2O_3 (versus 19,532 mmol gPd^{-1} h^{-1} for comparable loading Pd/SBA-16), consistent with the superior stabilisation of surface PdO evidenced in Table 1. In order to confirm that PdO is the active surface species responsible for cinnamyl alcohol selox over Pd-meso-Al_2O_3, as is known for Pd/silicas [6] and [7] and colloidal Pd nanoparticles [12] and [14], these initial selox activities were normalised to the surface concentration of PdO (derived from XPS) or Pd metal (derived from CO chemisorption) in order to calculate TOFs with respect to either potential active species. Fig. 3 reveals a constant TOF across the Pd-meso-Al_2O_3 family upon normalisation to surface PdO, entirely consistent with a common oxide active phase independent of loading, precisely as report for silica supports [6] and [7]. However, it is interesting to note that the TOF value for cinnamyl alcohol selox of ~ 14,100 h^{-1} for meso-Al_2O_3 supported palladium nanoparticles far exceeds that of 5,800 h^{-1} for Pd/silicas, indicating important differences in their respective Pd-oxide interactions [36] and [37]. While it is conceptually interesting to consider whether palladium loadings below 0.05 wt% (the lowest explored in this work) may offer even higher activities, it is virtually impossible to reproducibly synthesise and accurately characterise solids with lower palladium concentrations; solids with such extreme dilutions are not amenable to analysis by laboratory XPS or XRD, and extremely challenging for synchrotron XAS or HRTEM.

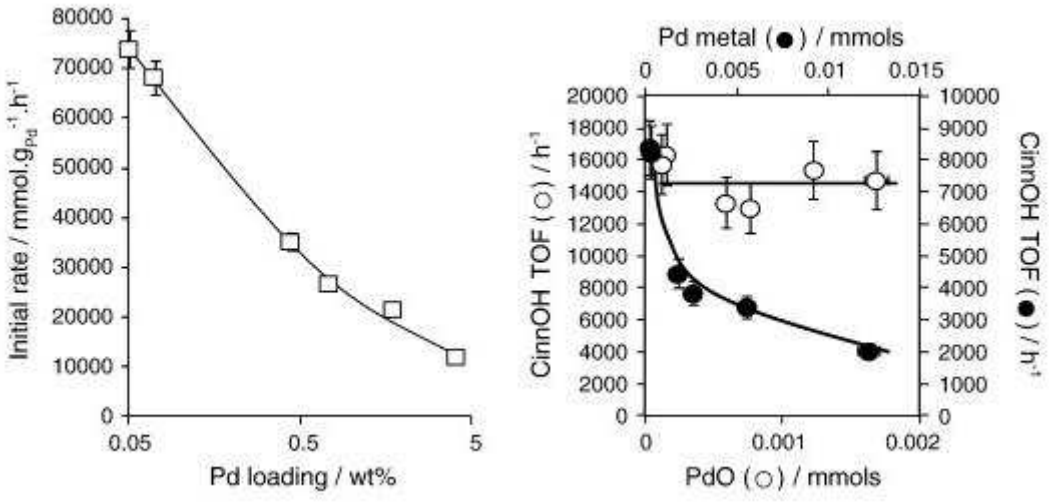

Fig. 3. (Left) Rate dependence of cinnamyl alcohol aerobic selox on bulk Pd loading for Pd/meso-Al_2O_3; and (right) corresponding cinnamyl alcohol aerobic selox TOFs as a function of surface PdO or Pd metal content.

Selectivity profiles for major products (> 1.5 % of total yield) are shown in Fig. 4 for representative low and high loading Pd/meso-Al_2O_3 catalysts. The principal product was cinnamaldehyde throughout reactions, with smaller amounts of 3-phenylpropan-1-ol formed via cinnamyl alcohol hydrogenation, and ethylbenzene, styrene and trans-β-methylstyrene (in a 1:1:1 ratio) via hydrogenolysis [38]. Cinnamaldehyde selectivity exhibited a rapid, but small, initial decrease during the first hour of reaction, which we attribute to in situ reduction of a small fraction of surface PdO to metal by hydrogen liberated during cinnamyl alcohol adsorption and subsequent dehydrogenation [6], [7], [11], [12], [13] and [14]. Limiting cinnamaldehyde selectivities remained > 65 % after 24 h in all cases, but increased with the initial degree of surface oxidation, consistent with observations from single crystal Pd(111) [10] and PdO_x/Pd(111) [8] model surfaces that PdO

favours cinnamaldehyde desorption, while metallic palladium promotes competitive hydrogenation and decarbonylation.

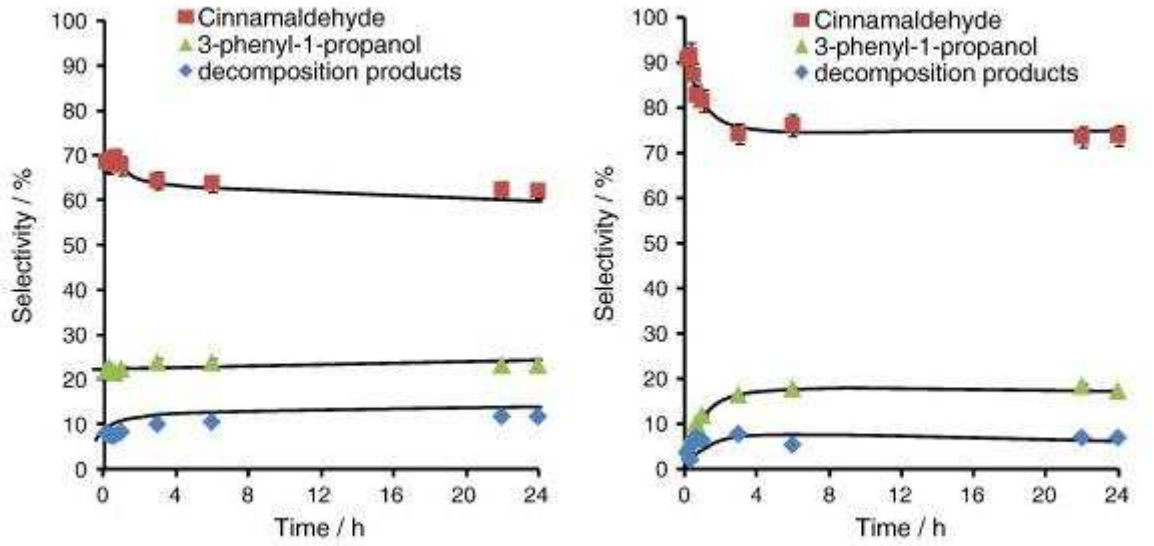

Fig. 4. Representative selectivity profiles for major products of cinnamyl alcohol selox over (left) 1.75 wt% Pd/meso-Al_2O_3 and (right) 0.05 wt% Pd/meso-Al_2O_3.

The stability of active sites was assessed post-reaction via XPS analysis of a spent 0.74 wt% Pd/meso-Al_2O_3 catalyst recovered from the reaction solution. Pd 3d XP spectra evidenced a small change in the concentration of surface PdO species with respect to the fresh catalyst as a result of in situ reduction after 24 h selox (Fig S4). This loss amounts to only 25 % of the initial surface PdO present in the as-prepared catalyst, and we attribute this as the primary origin for the loss in selectivity observed in Fig. 4. Some carbon deposition was also apparent in the corresponding C 1 s XP spectra (not shown), which may also contribute to lower cinnamaldehyde yields as a result of site-blocking. Despite these changes in surface composition, post-reaction catalysts could be readily recycled, an important consideration with respect to their commercialisation, by simple washing in toluene to achieve complete regeneration of their initial activity and selectivity (Fig S5). Such facile regeneration rules out any irreversible active site deactivation on-stream by e.g. palladium leaching, nanoparticle sintering or incorporation within the alumina matrix, or adsorption of strongly bound hydrocarbons or CO as a result of decarbonylation side reactions.

In order to evaluate to the wider potential of highly ordered mesoporous alumina as a preferred support for Pd catalysed allylic alcohol selox chemistry, the 0.74 wt% Pd/meso-Al_2O_3 sample was screened against a variety of primary, secondary and tertiary allylic alcohols, and benzyl alcohol, and benchmarked against similar Pd loadings (~ 0.8–0.9 wt%) on commercial γ-alumina, SBA-15 and KIT-6 supports (Table 2). Of the allylic substrates investigated, only linalool, a tertiary allylic alcohol, was unreactive, reflecting the absence of hydrogen bound to the β-carbon and higher activation barriers towards methyl C–H bond activation [39]. It is immediately apparent that initial selox rates for the 0.74 wt% Pd/meso-Al_2O_3 catalyst outperform those for the analogous amorphous γ-alumina support by at least a factor of two, and provides a 5–10 fold enhancement for crotyl and cinnamyl selox over mesoporous silica counterparts. Absolute rates scale inversely with molecular mass, decreasing in the order C_4 > C_5 ≈ benzyl alcohol > C_9 > C_{10} > > C_{15} as anticipated from the slower bulk and intra-pore diffusion (and greater steric constraints) of the bulkier

alcohols [40]. For all substrates, the TOFs indicate a common form of active surface PdO is present over both alumina supports, but which differs from that present in the (less active) Pd/SBA-15 and Pd/KIT-6 catalysts. We speculate that this difference arises from subtle changes in the local coordination environment of Pd^{2+} centres on alumina versus silica supports, which appear otherwise electronically indistinguishable by XPS. The desired allylic carbonyl products are always formed selectively, particularly allylic ketones for which selectivities exceed 97 %. In contrast, the 0.74 wt% Pd/meso-Al_2O_3 catalyst was ineffective towards a range of unactivated, saturated and non-allylic alcohols including 1-pentanol, cyclohexanol, 1-octanol, 2-octanol, 3-methyl-3-buten-1-ol, 2-phenylethanol and 3-phenyl-1-propanol, evidencing that the allylic functionality is critical role to the selox reaction. We postulate that this reflects stronger chemisorption (di-σ/π coordination) of the allylic function to the oxidised surface of palladium and weaker C-H bond of the allylic β carbon, that in concert serve to preferentially stabilise and activate allylic alcohols [10] under our reaction conditions which are significantly 'greener' in respect of lower temperature and pressure than comparative selox literature.

Alcohol	Support	Time /h	Conversion /%	Selectivity /%	Initial rate /mmolgPd^{1} h^{-1}	TOF (PdO) /h^{-1}
Crotyl alcohol	meso-Al_2O_3	1	61	55	33,237	17,389
	γ-alumina	1	43	49	18,228	17,641
	SBA-15	1	11	72	3020	6253
	KIT-6	1	18	67	6237	6303
3-buten-2-ol	meso-Al_2O_3	0.5	82	98	10,3111	53,946
	γ-alumina	0.5	69	99	54,357	52,608
Prenol	meso-Al_2O_3	1	57	67	29,252	15,304
	γ-alumina	1	38	68	14,647	14,176
3-penten-2-ol	meso-Al_2O_3	1	57	97	30,348	15,878
	γ-alumina	1	44	98	16,601	16,066
2-hexen-1-ol	meso-Al_2O_3	3	40	57	21,573	11,287
	γ-alumina	3	29	55	11,718	11,341
Benzyl alcohol	meso-Al_2O_3	1	70	97	31,811	16,643
	γ-alumina	1	55	93	16,275	15,751
Cinnamyl alcohol	meso-Al_2O_3	3	100	66	25,595	13,391
	γ-alumina	3	76	65	13,671	13,231
	SBA-15	3	40	78	2950	6108
	KIT-6	3	47	79	5782	5843
Trans-2-methyl-3-phenyl-2	meso-Al_2O_3	3	77	76	21,171	11,076
	γ-alumina	3	48	72	10,415	10,081
Geraniol (a)	meso-Al_2O_3	3	13	62	2011	1052
	γ-alumina	3	12	57	1075	1040
Farensol (a)	meso-Al_2O_3	5	12	70	731	425
	γ-alumina	5	11	65	439	383

Table 2. Comparative aerobic selox of allylic alcohols over alumina and silica supported Pd nanoparticles. (a) 100 mg catalyst employed.

4. Conclusions

The use of highly organised mesoporous alumina produced via EISA synthesis as a support for Pd nanoparticles affords exceptionally active and highly selective catalysts for the atom efficient, aerobic oxidation of allylic alcohols to aldehydes/ketones under mild reaction conditions. A strong palladium-alumina interaction helps to stabilise highly dispersed (0.8–2 nm) nanoparticles, which possess high concentrations of surface PdO even at bulk loadings of 4 wt%. Kinetic analysis confirms surface PdO as the catalytically active species responsible for allylic alcohol selox, with rates that exceed those over commercial alumina or analogous mesoporous silica supports.

Acknowledgements

The authors wish to thank the EPSRC (EP/E046754/1; EP/G007594/2; EP/F009488/1) for a Leadership Fellowship (AFL) and the Royal Society for an Industry Fellowship (KW). TEM was provided through the Leeds EPSRC Nanoscience and Nanotechnology Research Equipment Facility (LENNF) (EP/F056311/1).

References

[1] J.H. Clark. Green Chemistry: Challenges and Opportunities. Green Chemistry, 1 (1999), pp. 1–8.

[2] C.P. Vinod, K. Wilson, A.F. Lee. Recent advances in the heterogeneously catalysed aerobic selective oxidation of alcohols. Journal of Chemical Technology and Biotechnology, 86 (2011), pp. 161–171.

[3] G.O. Onawunmi. Evaluation of the antimicrobial activity of citral. Letters in Applied Microbiology, 9 (1989), pp. 105–108.

[4] T. Hattori, Y. Suzuki, O. Uesugi, S. Oi, S. Miyano. Cationic palladium(II) complex-catalyzed [2 + 2] cycloaddition and tandem cycloaddition-allylic rearrangement of ketene with aldehydes: an improved synthesis of sorbic acid. Chemical Communications (2000), pp. 73–74.

[5] C. Mercier, P. Chabardes. Organometallic chemistry in industrial vitamin-A and vitamin-E synthesis. Pure and Applied Chemistry, 66 (1994), pp. 1509–1518.

[6] C.M.A. Parlett, D.W. Bruce, N.S. Hondow, A.F. Lee, K. Wilson. Support-enhanced selective aerobic alcohol oxidation over Pd/mesoporous silicas. ACS Catalysis, 1 (2011), pp. 636–640.

[7] C.M.A. Parlett, D.W. Bruce, N.S. Hondow, M.A. Newton, A.F. Lee, K. Wilson. Mesoporous silicas as versatile supports to tune the palladium-catalyzed selective aerobic oxidation of allylic alcohols. ChemCatChem, 5 (2013), pp. 939–950.

[8] A.F. Lee, J.N. Naughton, Z. Liu, K. Wilson. High-pressure XPS of crotyl alcohol selective oxidation over metallic and oxidized Pd(111). ACS Catalysis, 2 (2012), pp. 2235–2241.

[9] J. Naughton, A. Pratt, C.W. Woffinden, C. Eames, S.P. Tear, S.M. Thompson, A.F. Lee, K. Wilson. Metastable de-excitation spectroscopy and density functional theory study of the selective oxidation of crotyl alcohol over Pd(111). Journal of Physical Chemistry C, 115 (2011), pp. 25290–25297.

[10] A.F. Lee, Z. Chang, P. Ellis, S.F.J. Hackett, K. Wilson. Selective oxidation of crotyl alcohol over Pd(111). Journal of Physical Chemistry C, 111 (2007), pp. 18844–18847.

[11] A.F. Lee, K. Wilson. Structure-reactivity correlations in the selective aerobic oxidation of cinnamyl alcohol: in situ XAFS. Green Chemistry, 6 (2004), pp. 37–42.

[12] A.F. Lee, C.V. Ellis, J.N. Naughton, M.A. Newton, C.M.A. Parlett, K. Wilson. Reaction-driven surface restructuring and selectivity control in allylic alcohol catalytic aerobic oxidation over Pd. Journal of the American Chemical Society, 133 (2011), pp. 5724–5727.

[13] C.M.A. Parlett, C.V. Gaskell, J.N. Naughton, M.A. Newton, K. Wilson, A.F. Lee. Operando synchronous DRIFTS/MS/XAS as a powerful tool for guiding the design of Pd catalysts for the selective oxidation of alcohols. Catalysis Today, 205 (2013), pp. 76–85.

[14] C.V. Gaskell, C.M.A. Parlett, M.A. Newton, K. Wilson, A.F. Lee. Redox-controlled crotyl alcohol selective oxidation: in situ oxidation and reduction dynamics of catalytic Pd nanoparticles via synchronous XANES/MS. ACS Catalysis, 2 (2012), pp. 2242–2246.

[15] A.P. Kumar, B.P. Kumar, A.B.V.K. Kumar, B.T. Huy, Y.-I. Lee. Preparation of palladium nanoparticles on alumina surface by chemical co-precipitation method and catalytic applications. Applied Surface Science, 265 (2013), pp. 500–509.

[16] T. Balcha, J.R. Strobl, C. Fowler, P. Dash, R.W.J. Scott. Selective aerobic oxidation of crotyl alcohol using AuPd core-shell nanoparticles. ACS Catalysis, 1 (2011), pp. 425–436.

[17] T. Hara, M. Ishikawa, J. Sawada, N. Ichikuni, S. Shimazu. Creation of highly stable monomeric Pd(II) species in an anion-exchangeable hydroxy double salt interlayer: application to aerobic alcohol oxidation under an air atmosphere. Green Chemistry, 11 (2009), pp. 2034–2040.

[18] G.-J.t. Brink, I.W.C.E. Arends, R.A. Sheldon. Green, catalytic oxidation of alcohols in water. Science, 287 (2000), pp. 1636–1639.

[19] B.A. Steinhoff, S.S. Stahl. Ligand-modulated palladium oxidation catalysis: mechanistic insights into aerobic alcohol oxidation with the $Pd(OAc)_2$/pyridine catalyst system. Organic Letters, 4 (2002), pp. 4179–4181.

[20] B. Feng, Z. Hou, X. Wang, Y. Hu, H. Li, Y. Qiao. Selective aerobic oxidation of styrene to benzaldehyde catalyzed by water-soluble palladium(II) complex in water. Green Chemistry, 11 (2009), pp. 1446–1452.

[21] L.J. Durndell, C.M.A. Parlett, N.S. Hondow, K. Wilson, A.F. Lee. Tunable Pt nanocatalysts for the aerobic selox of cinnamyl alcohol. Nanoscale, 5 (2013), pp. 5412–5419.

[22] Z.C. Ma, H.Q. Yang, Y. Qin, Y.J. Hao, G.A. Li. Palladium nanoparticles confined in the nanocages of SBA-16: enhanced recyclability for the aerobic oxidation of alcohols in water. Journal of Molecular Catalysis A: Chemical, 331 (2010), pp. 78–85.

[23] B. Karimi, A. Zamani, S. Abedia, J.H. Clark. Aerobic oxidation of alcohols using various types of immobilized palladium catalyst: the synergistic role of functionalized ligands, morphology of support, and solvent in generating and stabilizing nanoparticles. Green Chemistry, 11 (2009), pp. 109–119.

[24] Y. Chen, Z. Guo, T. Chen, Y. Yang. Surface-functionalized TUD-1 mesoporous molecular sieve supported palladium for solvent-free aerobic oxidation of benzyl alcohol. Journal of Catalysis, 275 (2010), pp. 11–24.

[25] S.E.J. Hackett, R.M. Brydson, M.H. Gass, I. Harvey, A.D. Newman, K. Wilson, A.F. Lee. High-activity, single-site mesoporous Pd/Al_2O_3 catalysts for selective aerobic oxidation of allylic alcohols. Angewandte Chemie International Edition, 46 (2007), pp. 8593–8596.

[26] J. Chen, Q.H. Zhang, Y. Wang, H.L. Wan. Size-dependent catalytic activity of supported palladium nanoparticles for aerobic oxidation of alcohols. Advanced Synthesis and Catalysis, 350 (2008), pp. 453–464.

[27] F. Vaudry, S. Khodabandeh, M.E. Davis. Synthesis of pure alumina mesoporous materials. Chemistry of Materials, 8 (1996), pp. 1451–1464.

[28] P. Yang, D. Zhao, D.I. Margolese, B.F. Chmelka, G.D. Stucky. Generalized syntheses of large-pore mesoporous metal oxides with semicrystalline frameworks. Nature, 396 (1998), pp. 152–155.

[29] Q. Yuan, A.X. Yin, C. Luo, L.D. Sun, Y.W. Zhang, W.T. Duan, H.C. Liu, C.H. Yan. Facile synthesis for ordered mesoporous γ-aluminas with high thermal stability. Journal of the American Chemical Society, 130 (2008), pp. 3465–3472.

[30] M. Kuemmel, D. Grosso, C. Boissière, B. Smarsly, T. Brezesinski, P.A. Albouy, H. Amenitsch, C. Sanchez. Thermally stable nanocrystalline γ-alumina layers with highly ordered 3D mesoporosity. Angewandte Chemie International Edition, 44 (2005), pp. 4589–4592.

[31] Q. Wu, F. Zhang, J. Yang, Q. Li, B. Tu, D. Zhao. Synthesis of ordered mesoporous alumina with large pore sizes and hierarchical structure. Microporous and Mesoporous Materials, 143 (2011), pp. 406–412.

[32] S.M. Morris, P.F. Fulvio, M. Jaroniec. Ordered mesoporous alumina-supported metal oxides. Journal of the American Chemical Society, 130 (2008), pp. 15210–15216.

[33] W. Cai, J. Yu, C. Anand, A. Vinu, M. Jaroniec. Facile synthesis of ordered mesoporous alumina and alumina-supported metal oxides with tailored adsorption and framework properties. Chemistry of Materials, 23 (2011), pp. 1147–1157.

[34] J.-P. Dacquin, J.r.m. Dhainau, D. Duprez, S.b Royer, A.F. Lee, K. Wilson. An efficient route to highly organized, tunable macroporous − mesoporous alumina. Journal of the American Chemical Society, 131 (2009), pp. 12896–12897.

[35] C.H. Bartholomew. Mechanisms of catalyst deactivation. Applied Catalysis A: General, 212 (2001), pp. 17–60.

[36] H. Dropsch, M. Baerns. CO adsorption on supported Pd catalysts studied by adsorption microcalorimetry and temperature programmed desorption. Applied Catalysis a-General, 158 (1997), pp. 163–183.

[37] A.Y. Stakheev, L.M. Kustov. Effects of the support on the morphology and electronic properties of supported metal clusters: modern concepts and progress in 1990s. Applied Catalysis a-General, 188 (1999), pp. 3–35.

[38] T. Mallat, A. Baiker. Oxidation of alcohols with molecular oxygen on solid catalysts. Chemical Reviews, 104 (2004), pp. 3037–3058.

[39] X.Y. Liu, R.J. Madix, C.M. Friend. Unraveling molecular transformations on surfaces: a critical comparison of oxidation reactions on coinage metals. Chemical Society Reviews, 37 (2008), pp. 2243–2261.

[40] P. Zhang, Y. Gong, H. Li, Z. Chen, Y. Wang. Solvent-free aerobic oxidation of hydrocarbons and alcohols with Pd@ N-doped carbon from glucose. Nature Communications, 4 (2013), p. 1593.